Synthesis, Characterization, and Self-Organization of Dendrimer-Encapsulated HgTe Quantum Dots

ARTICLE *in* LANGMUIR · JULY 2010

Impact Factor: 4.46 · DOI: 10.1021/la100866z · Source: PubMed

3 AUTHORS:

Amiya Priyam
Central University of Bihar
28 PUBLICATIONS **450** CITATIONS
SEE PROFILE

Daniel E Blumling
James Madison University
12 PUBLICATIONS **108** CITATIONS
SEE PROFILE

Kenneth L Knappenberger
Florida State University
61 PUBLICATIONS **540** CITATIONS
SEE PROFILE

Langmuir
Article
pubs.acs.org/Langmuir

Synthesis, Characterization, and Self-Organization of Dendrimer-Encapsulated HgTe Quantum Dots

Amiya Priyam, Daniel E. Blumling, and Kenneth L. Knappenberger, Jr.*

Department of Chemistry and Biochemistry, Florida State University, Tallahassee, Florida 32306

Received March 1, 2010. Revised Manuscript Received May 3, 2010

Mercury telluride (HgTe) quantum dots (QDs) were synthesized in methanol at 5 °C using generation 5 (G5) and 7 (G7) polyamidoamine (PAMAM) dendrimers, which function both as nucleation sites and as nanoparticle stabilizers. Transmission electron microscopy (TEM) data indicate these particles were slightly oblate, with an average aspect ratio of 1.3 ± 0.1 and a minor axis of 2.6 ± 0.3 nm. The crystal phase was determined to be coloradoite (cubic system) by analysis of the electron diffraction pattern. Absorption maxima for HgTe QDs ranged from 950 to 970 nm, depending on the dendrimer generation and concentration. QD size distribution was optimized by careful variation of the Hg^{2+}:dendrimer surface group molar ratio for both G5 and G7 dendrimers. An increase in molar ratio from 1:0.5 to 1:4 resulted in a decrease in the half-width at half-maximum (HWHM) of the HgTe bandgap absorption from 68 ± 3 to 52 ± 2 nm, indicating a size distribution focusing of 23 ± 4%. Second-derivative analysis of HgTe QD FTIR absorption spectra suggested that the quantum dots were fully encapsulated by a single G7 dendrimer, whereas multiple G5 dendrimers were necessary to stabilize a single nanoparticle. TEM and FTIR data revealed that the HgTe QDs form two-dimensional necklace-type arrays through a self-organization process, which proceeds through interpenetration of dendritic arms. TEM data further indicated that the average nanonecklace contained 10−15 QDs with an average inter-QD separation of 1.3 ± 0.7 nm and a total chain length of 46 ± 6 nm.

1. Introduction

Mercury chalcogenides represent a technologically important class of near-infrared (NIR) materials. Bulk mercury telluride (HgTe) is a semimetal with a negative band gap of −0.15 eV at room temperature and has one of the largest Bohr exciton diameters (80 nm) among II−VI semiconductors.[1−3] Nanocrystalline HgTe undergoes a semimetal to semiconductor transformation for particle sizes smaller than 18 nm,[2] providing an opportunity to study quantum confinement effects in small to large nanoparticles. Devices based on the NIR quantum dot (QD) platform are expected to impact areas such as solar-to-electric energy conversion,[4] optoelectronic and light-emitting devices,[1,5−9] photonics,[10] and several sensing applications.[11] Recent interest in developing photovoltaics that utilize NIR QDs stems from findings that indicate that solar light harvesting efficiency for these particles is significantly enhanced relative to that of similar devices that operate in the visible frequency range.[6,12] In addition, NIR nanoparticles may allow for improved biological imaging methods since they have potential to provide greater image penetration depths and function in the higher-transparency window of water.[6,13,14]

Creation of devices based on these technologies requires development of controlled and cost-effective methods to produce NIR QDs that are characterized by narrow size distributions and long-term stability. Many challenges still remain in achieving size- and shape-controlled synthesis of HgTe QDs. To date, the most successful route to HgTe QDs employs thiol capping in an aqueous medium.[3,5,15] However, the opaqueness of water at wavelengths of >1300 nm makes the optical characterization in aqueous solutions difficult. In general, mercury chalcogenides, as a class of materials, have been found to be difficult to prepare.[2,5,16] Therefore, a new method for HgTe QD synthesis is needed, a method that can provide improved control over the nucleation and growth processes while still allowing for optical characterization. Here, we present low-temperature (5 °C) dendrimer-mediated

*To whom correspondence should be addressed. E-mail: klk@chem.fsu.edu. Phone: (850) 645-8617. Fax: (850) 644-8281.

(1) Harrison, M. T.; Kershaw, S. V.; Burt, M. G.; Rogach, A. L.; Kornowski, A.; Eychmüller, A.; Weller, H. *Pure Appl. Chem.* **2000**, *72*, 295.
(2) Green, M.; Wakefield, G.; Dobson, P. J. *J. Mater. Chem.* **2003**, *13*, 1076.
(3) Rogach, A.; Kershaw, S.; Burt, M.; Harrison, M.; Kornowski, A.; Eychmuller, A.; Weller, H. *Adv. Mater.* **1999**, *11*, 552.
(4) (a) Kongkanand, A.; Tvrdy, K.; Takechi, K.; Kuno, M.; Kamat, P. V. *J. Am. Chem. Soc.* **2008**, *130*, 4007. (b) Robel, I.; Subramanian, V.; Kuno, M.; Kamat, P. V. *J. Am. Chem. Soc.* **2006**, *128*, 2385.
(5) Kovalenko, M. V.; Kaufmann, E.; Pachinger, D.; Roither, J.; Huber, M.; Stangl, J.; Hesser, G.; Schäffler, F.; Heiss, W. *J. Am. Chem. Soc.* **2006**, *128*, 3516.
(6) Sargent, E. H. *Adv. Mater.* **2005**, *17*, 515.
(7) Roither, J.; Kovalenko, M. V.; Pichler, S.; Schwarzl, T.; Heiss, W. *Appl. Phys. Lett.* **2005**, *86*, 241104.
(8) (a) Kershaw, S. V.; Harrison, M. T.; Burt, M. G. *Philos. Trans. R. Soc. London, Ser. A* **2003**, *361*, 331. (b) Stokes, E. B.; Stiff-Roberts, A. D.; Dameron, C. T. *Electrochem. Soc. Interface* **2006**, *15*, 23.
(9) Zhu, T.; Shanmugasundaram, K.; Price, S. C.; Ruzyllo, J.; Zhang, F.; Xu, J.; Mohney, S. E.; Zhang, Q.; Wang, A. Y. *Appl. Phys. Lett.* **2008**, *92*, 023111.
(10) Asakawa, K.; Sugimoto, Y.; Watanabe, Y.; Ozaki, N.; Mizutani, A.; Takata, Y.; Kitagawa, Y.; Ishikawa, H.; Ikeda, N.; Awazu, K.; Wang, X.; Watanabe, A.; Nakamura, S.; Ohkouchi, S.; Inoue, K.; Kristensen, M.; Sigmund, O.; Borel, P. I.; Baets, R. *New J. Phys.* **2006**, *8*, 208.
(11) (a) Michalet, X.; Pinaud, F. F.; Bentolila, L. A.; Tsay, J. M.; Doose, S.; Li, J. J.; Sundaresan, G.; Wu, A. M.; Gambhir, S. S.; Weiss, S. *Science* **2005**, *307*, 538. (b) Weng, J.; Ren, J. *Curr. Med. Chem.* **2006**, *13*, 897. (c) Smith, A. M.; Ruan, G.; Rhyner, M. N.; Nie, S. *Ann. Biomed. Eng.* **2006**, *34*, 3. (d) Pinaud, F.; Michalet, X.; Bentolila, L. A.; Tsay, J. M.; Doose, S.; Li, J. J.; Iyer, G.; Weiss, S. *Biomaterials* **2006**, *27*, 1679. (e) Bagalkot, V.; Zhang, L.; Levy-Nissenbaum, E.; Jon, S.; Kantoff, P. W.; Langer, R.; Farokhzad, O. C. *Nano Lett.* **2007**, *7*, 3065.
(12) McDonald, S. A.; Konstantatos, G.; Zhang, S.; Cyr, P. W.; Klem, E. J. D.; Levina, L.; Sargent, E. H. *Nat. Mater.* **2005**, *4*, 138.
(13) Cai, W.; Shin, D.-W.; Chen, K.; Gheysens, O.; Cao, Q.; Wang, S. X.; Gambhir, S. S.; Chen, X. *Nano Lett.* **2006**, *6*, 669.
(14) Kim, S.; Lim, Y. T.; Soltesz, E. G.; De Grand, A. M.; Lee, J.; Nakayama, A.; Parker, J. A.; Mihaljevic, T.; Laurence, R. G.; Dor, D. M.; Cohn, L. H.; Bawendi, M. G.; Frangioni, J. V. *Nat. Biotechnol.* **2004**, *22*, 93.
(15) Harrison, M. T.; Kershaw, S. V.; Rogach, A. L.; Kornowski, A.; Eychmuller, A.; Weller, H. *Adv. Mater.* **2000**, *12*, 123.
(16) Howes, P.; Green, M.; Johnston, C.; Crossley, A. *J. Mater. Chem.* **2008**, *18*, 3474.

synthesis in a nonaqueous solvent that yields stable, crystalline HgTe quantum dots. In addition, these quantum dots self-assemble and temporally evolve into short chainlike nanostructures.

Our synthetic strategy employed polyamidoamine (PAMAM) dendrimers, which are highly ordered three-dimensional, branched macromolecules.[17,18] The excellent coordinating ability of the interior amine and amide groups combined with the flexibility of the internal void space provides a well-defined nucleation center that can also function to stabilize metal[19−22] and semiconductor[23−26] nanoparticles. In this article, we report the low-temperature (5 °C) synthesis of dendrimer-encapsulated HgTe QDs in methanol. We determined the optimal nucleation temperature by exploring a range from 5 to 25 °C. Further, we elucidated the evolution of the pattern of binding of dendrimer functional groups to the HgTe particles by systematically varying the mercury ion:dendrimer molar ratios in two significantly different hosts, generation 5 (G5) and larger generation 7 (G7) PAMAM dendrimers. The former contains 128 surface amine groups, while the latter has 512. The HgTe QDs synthesized here exhibited absorption maxima in the range of 950−970 nm. The absorption maxima were controlled by careful optimization of the dendrimer generation and concentration. The patterns of binding between the nanoparticle surface and dendrimer functional groups were studied by analysis of the second derivative of the FTIR absorption spectra, providing details about conformational and vibrational changes in the dendrimer structure upon nanoparticle formation. Control over the size distribution in the dendrimer-mediated synthesis was achieved through a careful variation of the molar ratio of Hg^{2+} to surface groups of the dendrimer. We also report on the spontaneous organization of the HgTe quantum dots into two-dimensional arrays. The closely spaced HgTe QDs in these assemblies formed a chainlike structure resembling pearl necklace-type arrangements, which are hereafter termed nanonecklaces. These findings indicate that it is possible to develop novel methods of self-assembly of NIR QDs into two-dimensional (2D) or three-dimensional (3D) arrays without the need for external stimuli or templates. To date, most successful routes to nanoparticle assembly require templates such as DNA,[27,28] mesoporous silica,[29] or steps and edges supported on solid substrates.[30] Earlier, Zhang et al. fashioned nanonecklaces of CdS QDs using dendronized polymers.[31] Similar nanonecklaces of CdTe QDs were also synthesized without using such polymers, but they were unstable and transformed into nanowires.[32] When QDs assemble into nanowires, loss of confinement occurs in one direction; if they are organized into a necklace pattern, the individuality of the particles is retained, an attribute that may enable tailoring of nanostructure electronic coupling strength[33] and lead to efficient solar energy conversion. The advantage of our assembly technique is that a stable, free-floating necklace-type pattern can be obtained without the aid of chainlike polymeric structures.

2. Experimental Section

2.1. Materials. Anhydrous mercury(II) chloride (99.999%), polyamidoamine dendrimer, generation 5, ethylene diamine core [10% (w/v) in methanol], polyamidoamine dendrimer, generation 7, ethylene diamine core [5% (w/v) in methanol], sodium borohydride (98%), telluric acid (≥99%), and methanol (≥99.9%) were purchased from Sigma-Aldrich and used without further purification.

2.2. Methods. Dendrimer-encapsulated HgTe quantum dots were synthesized by reaction of mercury(II) chloride and NaHTe. The mercury precursor was formed when 27 mg of mercury(II) chloride was dissolved in 50 mL of methanol, yielding a 2 mM stock solution of Hg^{2+} ions. Three different sets of diluted G5 dendrimer solutions (2 mL) were prepared in methanol with concentrations of 3.9, 7.8, and 31.2 μM. Subsequently, 1 mL of the Hg^{2+} stock solution was added to each of the 2 mL dendrimer solutions. Since the PAMAM G5 dendrimer contains 128 surface groups, the molar ratios of Hg^{2+} to surface groups for these solutions are 1:0.5, 1:1, and 1:4. The Hg^{2+}/dendrimer solutions were held at a constant temperature (5 °C) and bubbled with nitrogen for 30 min. We note that 5 °C was determined to be the optimal nucleation temperature. We conducted the protocol as described at 10, 20, and 25 °C. The particles obtained from the synthesis conducted at 5 °C provided the highest quality and the most discrete exciton absorption peak, as shown in Figure S1 of the Supporting Information.

An aqueous solution of NaHTe was prepared by reduction of telluric acid with sodium borohydride. Telluric acid (20 mg) was dissolved in 2 mL of water, and 23 μL of the solution was further diluted with 100 μL of water. The diluted solution of telluric acid was heated, and a 2 M $NaBH_4$ solution was added dropwise under a continuous nitrogen flow. The color of the solution changed in the following order: colorless (H_6TeO_6) → black (Te) → purple (Te_2^{2-}) → colorless (Te^{2-}). The addition of $NaBH_4$ was discontinued upon observation of the final color change from purple to colorless. The solution was held at a constant temperature of 5 °C for 30 min.

An aliquot of the final NaHTe solution was injected into each of the Hg^{2+}/dendrimer solutions and maintained at 5 °C with vigorous stirring. The final Hg^{2+}:Te^{2-} molar ratio in the reaction mixture was 1:0.5. The solutions were stirred for 10 min to achieve dendrimer encapsulation of HgTe quantum dots. The influence of dendrimer generation on nanoparticle formation and stability was tested using four different concentrations of G7 dendrimers. Solutions (2 mL each) with concentrations of 0.98, 1.46, 1.95, and 7.8 μM were prepared. Addition of Hg^{2+} ions and the NaHTe solution was conducted as described above for G5 dendrimers. The PAMAM G7 dendrimer contains 512 surface amine groups, and therefore, the Hg^{2+}:surface group molar ratios for the Hg^{2+}/G7 dendrimer solutions were 1:0.5, 1:0.75, 1:1, and 1:4. The G7 dendrimer-encapsulated HgTe QDs prepared using a Hg^{2+}:surface group ratio of 1:4 had self-assembled into nanonecklaces following storage in the dark at 10 °C for 3 weeks.

UV−vis−NIR spectra of the samples were recorded on a Perkin-Elmer Lambda 950 spectrophotometer. FTIR measurements were taken using the Perkin-Elmer Spectrum 100 FTIR spectrometer operated in attenuated total reflectance (ATR) mode. Spectra were recorded in the range of 650−4000 cm^{-1},

(17) Tomalia, D. A.; Naylor, A. M.; Goddard, W. A., III *Angew. Chem., Int. Ed.* **1990**, *29*, 138.
(18) Frechet, J. M. J.; Tomalia, D. A. *Dendrimers and Other Dendritic Polymers*; Lavoisier: Paris, 2001.
(19) Crooks, R. M.; Zhao, M.; Sun, L.; Chechik, V.; Yeung, L. K. *Acc. Chem. Res.* **2001**, *34*, 181.
(20) Scott, R. W. J.; Wilson, O. M.; Crooks, R. M. *J. Phys. Chem. B* **2005**, *109*, 692.
(21) Knecht, M. R.; Weir, M. G.; Frenkel, A. I.; Crooks, R. M. *Chem. Mater.* **2008**, *20*, 1019.
(22) Knecht, M. R.; Crooks, R. M. *New J. Chem.* **2007**, *31*, 1349.
(23) Wu, X. C.; Bittner, A. M.; Kern, K. *J. Phys. Chem. B* **2005**, *109*, 230.
(24) Lakowicz, J. R.; Gryczynski, I.; Piszczek, G.; Murphy, C. J. *J. Phys. Chem. B* **2002**, *106*, 5365.
(25) Ghosh, S.; Priyam, A.; Chatterjee, A.; Saha, A. *J. Nanosci. Nanotechnol.* **2008**, *8*, 5952.
(26) Ghosh, S.; Priyam, A.; Saha, A. *J. Nanosci. Nanotechnol.* **2009**, *9*, 6726.
(27) Sharma, J.; Chhabra, R.; Liu, Y.; Ke, Y.; Yan, H. *Angew. Chem., Int. Ed.* **2006**, *45*, 730.
(28) Nykypanchuk, D.; Maye1, M. M.; van der Lelie, D.; Gang, O. *Nature* **2008**, *451*, 549.
(29) Yan, W.; Chen, B.; Mahurin, S. M.; Hagaman, E. W.; Dai, S.; Overbury, S. H. *J. Phys. Chem. B* **2004**, *108*, 2793.
(30) Huang, J.; Tao, A. R.; Connor, S.; He, R.; Yang, P. *Nano Lett.* **2006**, *6*, 525.
(31) Zhang, Y.; Chen, Y.; Niu, H.; Gao, M. *Small* **2006**, *2*, 1314.
(32) Tang, Z.; Kotov, N. A.; Giersig, M. *Science* **2002**, *297*, 237.
(33) Williams, K. J.; Tisdale, W. A.; Leschkies, K. S.; Haugstad, G.; Norris, D. J.; Aydil, E. S.; Zhu, X.-Y. *ACS Nano* **2009**, *3*, 1532.

with a resolution of 2 cm^{-1}. For transmission electron microscopy (TEM), two or three drops of the samples were placed on the carbon-coated copper grid, and excess solvent was immediately evaporated. These samples were then analyzed with a JEOL-2010 transmission electron microscope, and the images were recorded at an operating voltage of 200 kV.

3. Results and Discussion

Dendrimer-mediated synthesis of HgTe nanocrystals was conducted using G5 and G7 PAMAM dendrimers in methanol at 5, 10, 20, and 25 °C. The temperature, 5 °C, was optimized for the syntheses as it yielded nanocrystals having a narrow size distribution and a distinct excitonic peak. At higher temperatures, the absorption spectra of HgTe quantum dots were extremely broad, indicating poor monodispersity of the nanocrystals, as shown in Figure S1 of the Supporting Information. NaHTe was prepared by reduction of telluric acid with $NaBH_4$ and was subsequently added to the N_2-purged solution of dendrimer and Hg^{2+} ions. The solution then turned golden brown, signifying the formation of HgTe nanocrystals, which was subsequently confirmed by selected area electron diffraction. The effects of the Hg^{2+}:dendrimer molar ratio and reagent concentration were investigated as discussed below. The majority of the studies were conducted using HgTe QDs synthesized using the G7 dendrimer because of the increased stability of this sample. In the final section, we also present a unique self-organizing behavior of these dendrimer-encapsulated QDs that can be utilized to devise a simple technique to make one-dimensional (1D) and 2D nanostructures. Surprisingly, these QDs did not exhibit luminescence, possibly because of the strong quenching effect of amine groups in the dendrimer.[34]

3.1. Dendrimer Encapsulation of HgTe QDs. The Hg^{2+}:dendrimer molar ratio was systematically increased to determine the ideal synthetic parameters for achieving stable and monodisperse HgTe QDs. PAMAM G5 dendrimers have 128 primary amine groups on the surface, 126 tertiary amine groups, and 252 amide groups in the interior;[19,20] both the outer primary and inner tertiary amine groups are available for transition metal ion coordination.[35−38] The concentration of dendrimers was varied to achieve Hg^{2+}:surface amine group molar ratios from 1:0.5 to 1:4. It should be noted that this value refers to the number of surface end groups only and does not imply any specific binding to these groups. Although the effect of loading ratios on the dendrimer-mediated synthesis of metal nanoparticles has been investigated previously,[19,20] information regarding metal ion loading factors for the formation of semiconductor particles in the dendrimer matrix is sparse.[39] The optical absorption spectra of HgTe nanoparticles formed at different Hg^{2+}:surface amine group molar ratios of the PAMAM dendrimer (G5) are shown in Figure 1a, and the absorption data are summarized in Table S1 of the Supporting Information. A distinct exciton absorption peak was observed for particles created under all synthetic conditions tested; however, the absorption peak became increasingly well-defined as the loading ratio of metal to dendrimer decreased. A gradual red shift of the exciton peak spectral position was also observed upon alteration of the ratio from 1:0.5 to 1:4. By

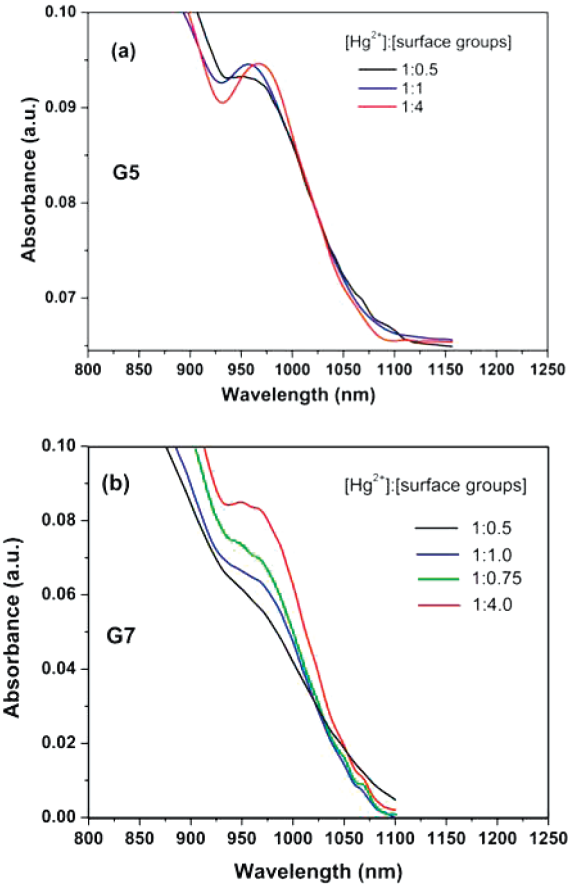

Figure 1. Near-infrared absorption of HgTe QDs prepared with G5 dendrimers (a) and G7 dendrimers (b) at different molar ratios of Hg^{2+} to surface groups of the dendrimer (5 °C, 0.66 mM Hg^{2+}, 128 and 512 surface groups in G5 and G7 dendrimers, respectively).

comparison, the change in the optical band gap (Table S1 of the Supporting Information) as calculated from the inflection point in the first-derivative plot was statistically insignificant.[40] This finding implied that the average particle size of the HgTe QDs was independent of the dendrimer concentration. This result was contrary to the "fixed loading law" [19,20,41]for metal nanoparticles, which predicts concomitant particle size and loading factor ([M^+]:[surface group]) decreases. However, there was a distinct reduction in the width of the first-exciton absorption peak with the gradual change in the Hg^{2+}:surface group molar ratio from 1:0.5 to 1:4. This shift indicated a narrowing of the nanoparticle size distribution. A similar reduction in absorption peak width is also observed by Gao et al.[31] for the synthesis of CdS nanoparticles with dendronized copolymers using different feed ratios. The well-established method of using the HWHM (half-width at half-maximum to the longer wavelength side of the first absorption peak) to index the nanoparticle size distribution was employed.[42] As shown in Table S1 of the Supporting

(34) (a) Ghosh, S.; Priyam, A.; Bhattacharya, S. C.; Saha, A. *J. Fluoresc.* **2009**, *19*, 723. (b) Pan, B.; Gao, F.; He, R.; Cui, D.; Zhang, Y. *J. Colloid Interface Sci.* **2006**, *297*, 151.
(35) Ottaviani, M. F.; Bossman, S.; Turro, N. J.; Tomalia, D. A. *J. Am. Chem. Soc.* **1994**, *116*, 661.
(36) Ottaviani, M. F.; Montalti, F.; Turro, N. J.; Tomalia, D. A. *J. Phys. Chem. B* **1997**, *101*, 158.
(37) Zhao, M.; Sun, L.; Crooks, R. M. *J. Am. Chem. Soc.* **1998**, *120*, 4877.
(38) Balogh, L.; Tomalia, D. A. *J. Am. Chem. Soc.* **1998**, *120*, 7355.
(39) Lemon, B. I.; Crooks, R. M. *J. Am. Chem. Soc.* **2000**, *122*, 12886.
(40) (a) Viswanatha, R.; Amenitsch, H.; Sarma, D. D. *J. Am. Chem. Soc.* **2007**, *129*, 4470. (b) Viswanatha, R.; Sarma, D. D. *Chem.—Eur. J.* **2006**, *12*, 180. (c) Nag, A.; Sapra, S.; Nagamani, C.; Sharma, A.; Pradhan, N.; Bhat, S. V.; Sarma, D. D. *Chem. Mater.* **2007**, *19*, 3252. (d) Priyam, A.; Ghosh, S.; Bhattacharya, S. C.; Saha, A. *J. Colloid Interface Sci.* **2009**, *333*, 195.
(41) Gröhn, F.; Bauer, B. J.; Akpalu, Y. A.; Jackson, C. L.; Amis, E. J. *Macromolecules* **2000**, *33*, 6042.
(42) (a) Yu, W. W.; Falkner, J. C.; Shih, B. S.; Colvin, V. L. *Chem. Mater.* **2004**, *16*, 3318. (b) Qu, L.; Yu, W. W.; Peng, X. *Nano Lett.* **2004**, *4*, 465. (c) Dai, Q.; Li, D.; Chang, J.; Song, Y.; Kan, S.; Chen, H.; Zou, B.; Xu, W.; Xu, S.; Liu, B.; Zou, G. *Nanotechnology* **2007**, *18*, 405603.

Information, the HWHM decreased from 68 ± 3 to 52 ± 2 nm when the molar ratio was altered from 1:0.5 to 1:4, suggesting a size distribution focusing of approximately 20−25%.

The HgTe nanoparticles synthesized with the PAMAM G5 dendrimer exhibited short-term (~24 h) stability preceding nanoparticle precipitation. Most likely, a single G5 dendrimer was not able to surround fully a single nanoparticle, since complete encapsulation of a single nanoparticle by one dendrimer typically results in good solution-phase stability.[19,20] In lower-generation dendrimers such as G5, a single host is likely too small[41] to passivate the surface of HgTe particles, thus resulting in hybrid structures in which multiple dendrimers are required to stabilize the quantum dots. This finding agrees well with previous results obtained for the synthesis of gold nanoparticles with lower-generation dendrimers.[41] Although the G5-based nanoparticles exhibited only short-term solution-phase stability, precipitated G5 HgTe QDs were readily redispersed upon sonication, and the absorption spectra (not shown) reproduced those of freshly prepared samples. The reproduction of the absorption spectrum obtained for the initial, nonaggregated dendrimer−HgTe particles indicated that the identity of the QDs was not compromised by precipitation. This suggested that the HgTe QDs remained stabilized by multiple dendrimers, and the dendrimer−HgTe composite particles had simply aggregated and settled out of solution rather than forming some other higher-order structure. Crystal−crystal aggregation of HgTe QDs could also be ruled out since this would have resulted in the well-known red shift[40,42] of the excitonic peak in the optical absorption measurements, an effect that was not observed for these samples.

The near-infrared absorption spectra of HgTe QDs synthesized using the G7 dendrimer are shown in Figure1b. A diffuse absorption feature was observed for the QDs prepared at a ratio of 1:0.5 ([M^+]:[dendrimer surface group]), likely because of a large distribution of particle sizes. At a loading factor of 1:4, the absorption profile improved substantially, and a peak around 955 nm appeared, suggesting decreased nanoparticle polydispersity.[40,42] TEM and electron diffraction (ED) measurements were performed on HgTe QDs synthesized with G7 dendrimers to determine the size and crystal structure of the nanoparticles. The data indicated that the nanoparticles were oblate spheroids with a minor axis and a major axis of 2.6 ± 0.3 and 3.3 ± 0.4 nm, respectively, and an aspect ratio of 1.3 ± 0.2 (Figure 2a,b). This analysis is consistent with previous fluorescence anisotropy measurements conducted on CdS and ZnS semiconducting nanoparticles grown in a dendrimer matrix, which yielded fluorescence properties indicative of an oblate structure.[24,26] The electron diffraction pattern shown in Figure 2c includes three bright rings. The observed *d* values of 3.7, 2.2, and 1.9 Å (lattice plane *hkl* values of 111, 220, and 311, respectively) suggested a coloradoite phase (cubic system) (JCPDS Card 75-2087).

All samples synthesized using G7 dendrimers were very stable and remained in suspension for more than 5 weeks. In fact, the sample synthesized using a loading factor of 1:4 was found to be exceptionally stable, with no sign of precipitation after 1 year. Thus, G7-synthesized QDs satisfy the precondition of nonprecipitation for encapsulation of a colloidal particle by a single dendrimer as identified in earlier work.[41] As indicated above, this result was in contrast with those obtained for QDs synthesized using G5 dendrimers, which did not meet this criterion.

As a confirmation of single-dendrimer encapsulation, and to understand further the binding of HgTe QDs to the functional groups of PAMAM G7 dendrimers, FTIR absorption data were collected for samples prepared at all loading factors. Representative FTIR spectra for the free G7 dendrimer as well as nanoparticles

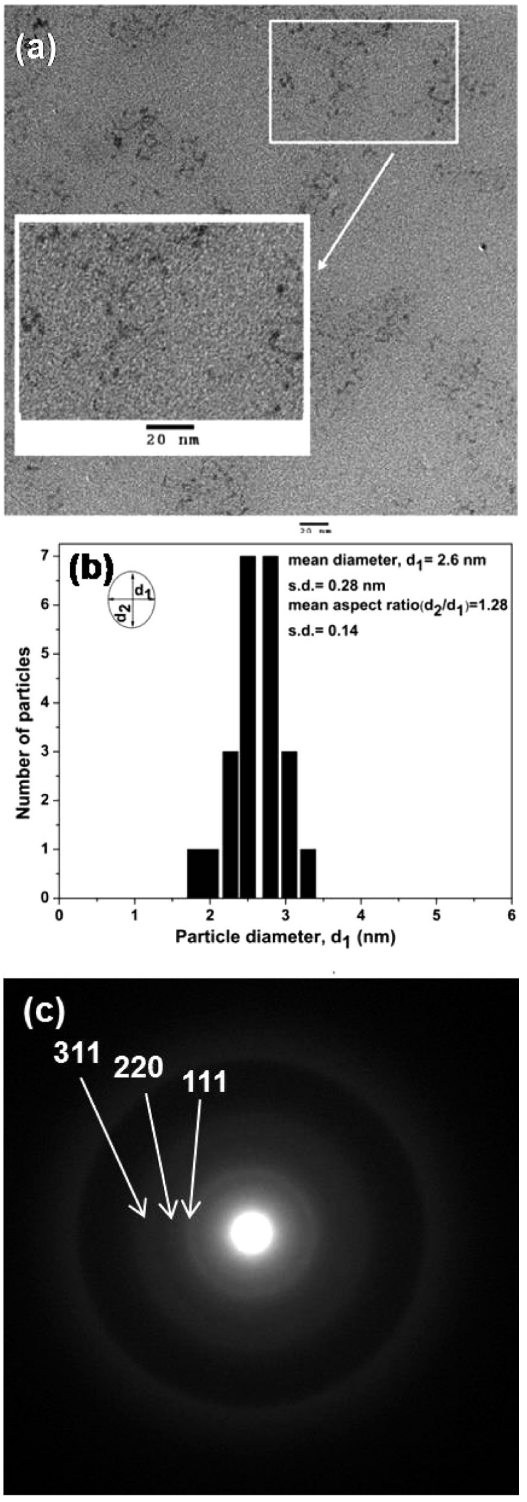

Figure 2. (a) TEM image of HgTe QDs prepared using G7 dendrimers at a Hg^{2+}:surface group molar ratio of 1:4. The inset is a zoomed-in view of a portion showing the size and shape of the particles. (b) Size distribution histogram derived from the TEM image. (c) Selected area electron diffraction (SAED) pattern (the three bright rings correspond to the 110, 220, and 311 *hkl* planes of colordoite-phase HgTe).

synthesized at all loading factors are shown in Figure 3. Four spectral features were readily apparent upon binding of the QD to the dendrimer: (i) the band at 1640 cm^{-1} shifted to 1630 cm^{-1} and became narrower; (ii) the band at 1555 cm^{-1} shifted to 1563 cm^{-1}; (iii) the band at 3282 cm^{-1} broadened considerably, and the peak

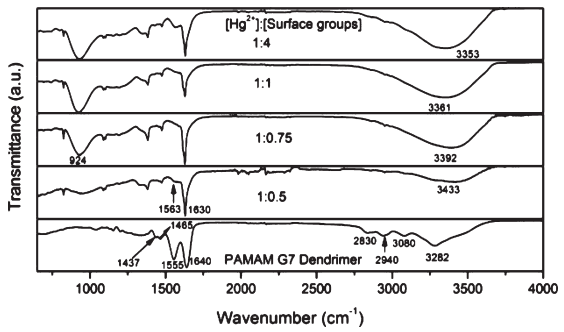

Figure 3. FTIR spectra of HgTe QDs synthesized using using G7 dendrimers at varying Hg^{2+}:surface group molar ratios.

shifted to higher energy as the dendrimer concentration was increased; and (iv) a new peak, which increased in amplitude for higher load factors, appeared at 924 cm^{-1}.

The FTIR absorption peaks were assigned as follows. The two broad peaks at 1640 and 1555 cm^{-1} were readily assigned to C═O stretching (amide I) and N−H bending/C−N stretching (amide II) vibrations of the dendrimer interior,[25,43] respectively. The 10 cm^{-1} red shift in the amide I frequency and the 8 cm^{-1} blue shift in the amide II frequency clearly indicated that the two interior functional groups were sensitive to the inclusion of the HgTe nanocrystals, suggesting that the dendrimer interior interacts directly with the HgTe nanoparticle surface. The effect of HgTe−dendrimer interactions was even more pronounced in amide I vibrations, which were considerably narrower in the nanoparticle spectra relative to the free dendrimer spectrum. The full width at half-maximum (fwhm) decreased from 50 to 30 cm^{-1} with the concomitant relative intensity increase. The ratio of the amide I to amide II peak areas increased from 3:2 for the native dendrimer to 6:1 and 8:1 for the dendrimer−HgTe QDs prepared at loading ratios of 1:4 and 1:0.5, respectively. Trends in the ratios of amide vibration peak areas are commonly used to analyze protein secondary structure.[43,44] Amide I and amide II vibrational frequencies depend upon local α-helical or β-strand conformations, which, in turn, are affected by the surrounding environment. The formation of HgTe nanoparticles in the void space of the dendrimer likely disrupts the hydrogen bonding interactions between the neighboring dendrimer branches, resulting in conformational changes. This assessment is further supported by the 40% reduction in the fwhm of amide I vibrations, as stated above. Although band broadening is a commonly observed phenomenon in systems involving dendrimer-encapsulated semiconductor and metal nanoparticles,[25,43] the narrowing effect reported here, to the best of our knowledge, has not been observed previously. The peak width of the vibrational bands contains information about rotational motion, and a reduction in fwhm is usually attributed to restricted rotation in the laboratory frame.[45] These results indicate that the occupancy of dendrimer void space by a HgTe particle caused a change in 3D conformation, and, thereby, restricted rotational motion, resulting in vibrational peak narrowing. Taken together, the data strongly suggest single-dendrimer encapsulation of HgTe QDs.

The lower-energy vibrations of the methylene groups, H−C−H scissor mode at 1465 cm^{-1} and H−C−H asymmetric deformations at 1437 cm^{-1}, exhibited shifts of 11 and 54 cm^{-1}, respectively. Previously, similar but smaller shifts were interpreted as a conformational change because of the adsorption of dendrimer branches onto the surface of gold and silver nanoparticles.[46] The larger shift observed in this case suggested a strong interaction, such as encapsulation of HgTe particles by dendrimers. The peak centered at 924 cm^{-1} in the dendrimer−HgTe system, which increased in amplitude with an increase in the dendrimer concentration, was assigned to the NH_2 wag + CH_2 rocking modes in PAMAM dendrimers, in agreement with theoretical predictions.[47] These vibrations are sensitive to local structure;[48] the absence of this peak in the FTIR spectrum obtained for the free dendrimer suggested that these vibrations were not supported in the native state. However, the rotomeric state populated by the dendrimer upon formation of HgTe particles allowed this vibration, and we observed a gradual enhancement in peak intensity with an increase in the number of such dendrimer-encapsulated HgTe units.

The band at 3282 cm^{-1} was assigned to the N−H stretching mode of dendrimer surface amine groups.[25,43,47] Relative to the spectrum of the free dendrimer, this peak broadened and exhibited blue shifts of 151, 110, 79, and 71 cm^{-1} for Hg^{2+}:surface group ratios of 1:0.5, 1:0.75, 1:1, and 1:4, respectively. This result indicated that the HgTe surface was also coordinated by some of the surface amines. When the dendrimer concentration is limiting, formation of nanoparticles that are only partially encapsulated can occur. In this situation, particle stability requires metal coordination by surface amines of multiple dendrimers. Such direct interactions between exterior NH_2 groups and the nanoparticle surface should result in large shifts in the frequency of the vibration peak, which was observed in the FTIR spectra of lower-ratio samples (1:0.5). As the dendrimer concentration was gradually increased, the number of particles stabilized via surface amines decreased, and therefore, the extent of the shift was reduced. When the ratio was 1:4, the spectral position of the peak corresponding to the N−H stretching mode approached that observed for the native dendrimer.

To gain further insight into the HgTe−dendrimer interactions, we rigorously analyzed the absorption peaks in the 3000−3700 cm^{-1} region, deconvoluting this portion of the spectrum into Gaussian functions. Location and identification of each modified dendrimer band in the congested spectral region were assessed using the second-derivative method;[49] the results are summarized in Table S2 of the Supporting Information. The second-derivative IR spectrum provides more details than the raw data and can be used to extract small differences between FTIR spectra. As shown in Figure 4a, the observed FTIR spectrum for the free dendrimer was resolved into six bands following deconvolution: 1,1′, overtone of amide II; 2,2′, H-bonded NH stretch; 3,3′, N−H symmetric stretch; 4,4′, N−H asymmetric stretch; 5,5′, amide A vibrations (N−H stretch of amide groups); 6,6′, O−H stretch (from solvent methanol).[47,49,50] The N−H stretch vibrations (3,3′ peaks) of the surface amines dominated the spectrum and accounted for nearly half of the total integrated intensity in the region of 3000−3700 cm^{-1} (Table S2 of the Supporting Information). However, the relative intensity of this peak decreased substantially upon formation of HgTe QDs, and two new peaks

(43) Liu, D.; Gao, J.; Murphy, C. J.; Williams, C. T. *J. Phys. Chem. B* **2004**, *108*, 12911.
(44) (a) van de Weert, M.; Haris, P. I.; Hennink, W. E.; Crommelin, D. J. A. *Anal. Biochem.* **2001**, *297*, 160. (b) Beekes, M.; Lasch, P.; Naumann, D. *Vet. Microbiol.* **2007**, *123*, 305. (c) Jackson, M.; Mantsch, H. H. *Can. J. Chem.* **1991**, *69*, 1639.
(45) (a) Sinnamon, B. F.; Dluhy, R. A.; Barnes, G. T. *Colloid Surf., A* **1999**, *156*, 215. (b) Frost, R. L. *Clay Clay Miner.* **1998**, *46*, 280.
(46) Manna, A.; Imae, T.; Aoi, K.; Okada, M.; Yogo, T. *Chem. Mater.* **2001**, *13*, 1674.
(47) Tarazona-Vasquez, F.; Balbuena, P. B. *J. Phys. Chem. B* **2004**, *108*, 15982.
(48) Olbert-Majkut, A.; Mielke, Z. *Phys. Chem. Chem. Phys.* **2006**, *8*, 4773.
(49) Popescu, M.-C.; Filip, D.; Vasile, C.; Cruz, C.; Rueff, J. M.; Marcos, M.; Serrano, J. L.; Singurel, G. *J. Phys. Chem. B* **2006**, *110*, 14198.
(50) Deutsch, D. S.; Siani, A.; Fanson, P. T.; Hirata, H.; Matsumoto, S.; Williams, C. T.; Amiridis, M. D. *J. Phys. Chem. C* **2007**, *111*, 4246.

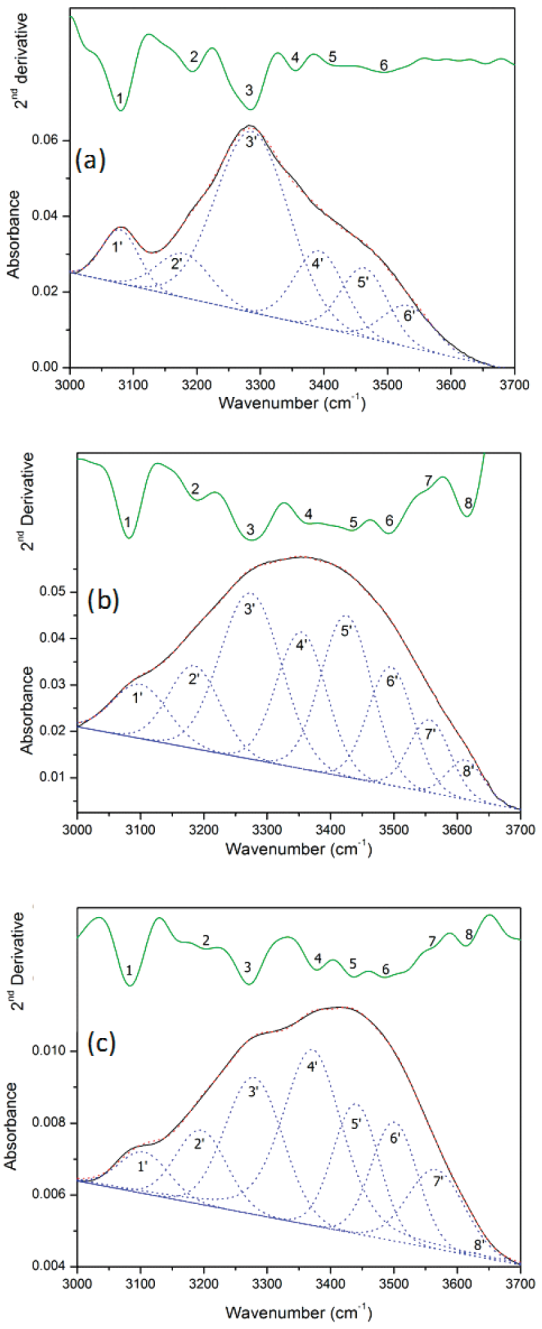

Figure 4. Deconvolution of FTIR spectra of the G7 dendrimer (a) and dendrimer−HgTe QDs at loading factors of 1:4 (b) and 1:0.5 (c) in the 3000−3700 cm^{-1} region: (black line) raw FTIR data, (blue dots) deconvoluted peaks, (red dots) overall fitting, and (green line) second-derivative plot. Band assignments of deconvolutions: 1,1′, overtone of amide II;[50] 2,2′, H-bonded N−H stretch;[49] 3,3′-N−H symmetric stretch;[43,47,49,50] 4,4′, N−H asymmetric stretch;[47] 5,5′, amide A vibrations (N−H stretch of amide);[47] 6,6′, O−H stretch;[49] 7,7′ and 8,8′, HgTe-bonded N−H stretch.

appeared in the second-derivative spectra at 3560 and 3615 cm^{-1} (Figure 4b,c). Since these peaks were absent in the FTIR spectra of both the free dendrimer and the Hg^{2+}-bound dendrimer, they were assigned to vibrations of NH_2 groups (symmetric and asymmetric stretch) coordinated to the HgTe surface. The appearance of these peaks was accompanied by a decrease in the relative intensity of the 3,3′ peak (N−H symmetric stretch), resulting in the overall shift of the broadened peak in the region. As the Hg^{2+}:surface group ratio was changed stepwise from 1:4 to 1:0.5, the decrease in the relative intensity of the 3,3′ peak became more pronounced, which, in turn, caused a larger shift in the originally broadened peak in the 3000−3700 cm^{-1} region. This effect clearly showed that the interaction between surface amines and HgTe particles was stronger at lower dendrimer concentrations, which are presumably insufficient for full nanoparticle encapsulation. When dendrimers are present at limiting concentrations and Hg^{2+} ions are in excess, some Hg^{2+} ions are likely to remain bonded to the surface amines rather than being coordinated by the interior functional groups of dendrimers. In these cases, the formation of HgTe particles occurs outside as well as inside the dendrimer cavity. The HgTe particles formed outside the void space of the dendrimer can therefore interact with surface groups of multiple dendrimers. This effect was observed as a greater decrease in the relative intensity of N−H stretch vibrations. Thus, optimization of the Hg^{2+}:dendrimer molar ratio is essential to ensure nucleation within the cavity and subsequent encapsulation of the nanoparticle.

3.2. Self-Organization of HgTe QDs. G7 dendrimer-encapsulated quantum dots prepared at a loading factor of 1:4 spontaneously organized into two-dimensional necklace-type arrays. The self-organization process occurred while the samples were stored in the dark at 10 °C over a period of 3 weeks. TEM images of the nanonecklaces are shown in Figure 5. Interparticle gaps are clearly evident in the TEM image shown in Figure 5a, as well as in the zoomed-in region shown in Figure 5b. In the high-resolution TEM image (Figure S2 of the Supporting Information), lattice fringes having an interplanar spacing of 3.7 Å (corresponding to 111 *hkl* planes of the coloradoite phase) can be seen, indicating that the crystal structure of the QDs was retained despite necklace formation. The distribution of chain lengths is represented by the histogram shown in Figure 5c. The average chain length was 46 ± 6 nm, demonstrating a narrow length distribution. Each nanonecklace consists of 12 ± 2 QDs separated by a distance of 1.3 ± 0.7 nm (Figure 5d,e). The near-infrared absorption spectra of the necklaces and freshly prepared quantum dots are shown in Figure 6. A small red shift (15 nm) of the excitonic peak (observed at 955 nm for QDs and 970 nm for nanonecklaces) and a concomitant 20 nm reduction in the HWHM were observed upon self-assembly of QDs into nanonecklaces. There are two possible explanations for the observed red shift: (i) growth in size of the QDs and (ii) an increase in inter-QD electronic coupling. The first possibility was ruled out because no significant change in QD size was apparent upon comparison of the TEM images of the individual QDs (Figure 2) and the self-assembled ones (Figure 5). Moreover, ripening of particles would lead to a broadening of the excitonic transition,[42,51] which was not observed in the case presented here. Therefore, the observed red shift was attributed to electronic coupling that resulted when the QDs closely approach each other during the self-assembly process. A similar red shift is also observed for PbSe QDs when the inter-QD separation was gradually reduced in a submonolayer thin film.[33] As the inter-QD separation decreases, the enhancement of the electronic exchange coupling energy likely arises from increased spatial overlap of the wave functions, which can lead to a red shift in the first exciton transition.

The mechanism of self-organization of QDs into 2D necklaces was examined to establish the dendrimer's role in this process. The

(51) (a) Gaponik, N.; Talapin, D. V.; Rogach, A. L.; Hoppe, K.; Shevchenko, E. V.; Kornowski, A.; Eychmüller, A.; Weller, H. *J. Phys. Chem. B* **2002**, *106*, 7177. (b) Peng, X.; Wickham, J.; Alivisatos, A. P. *J. Am. Chem. Soc.* **1998**, *120*, 5343. (c) Priyam, A.; Chatterjee, A.; Bhattacharya, S. C.; Saha, A. *J. Cryst. Growth* **2007**, *304*, 416.

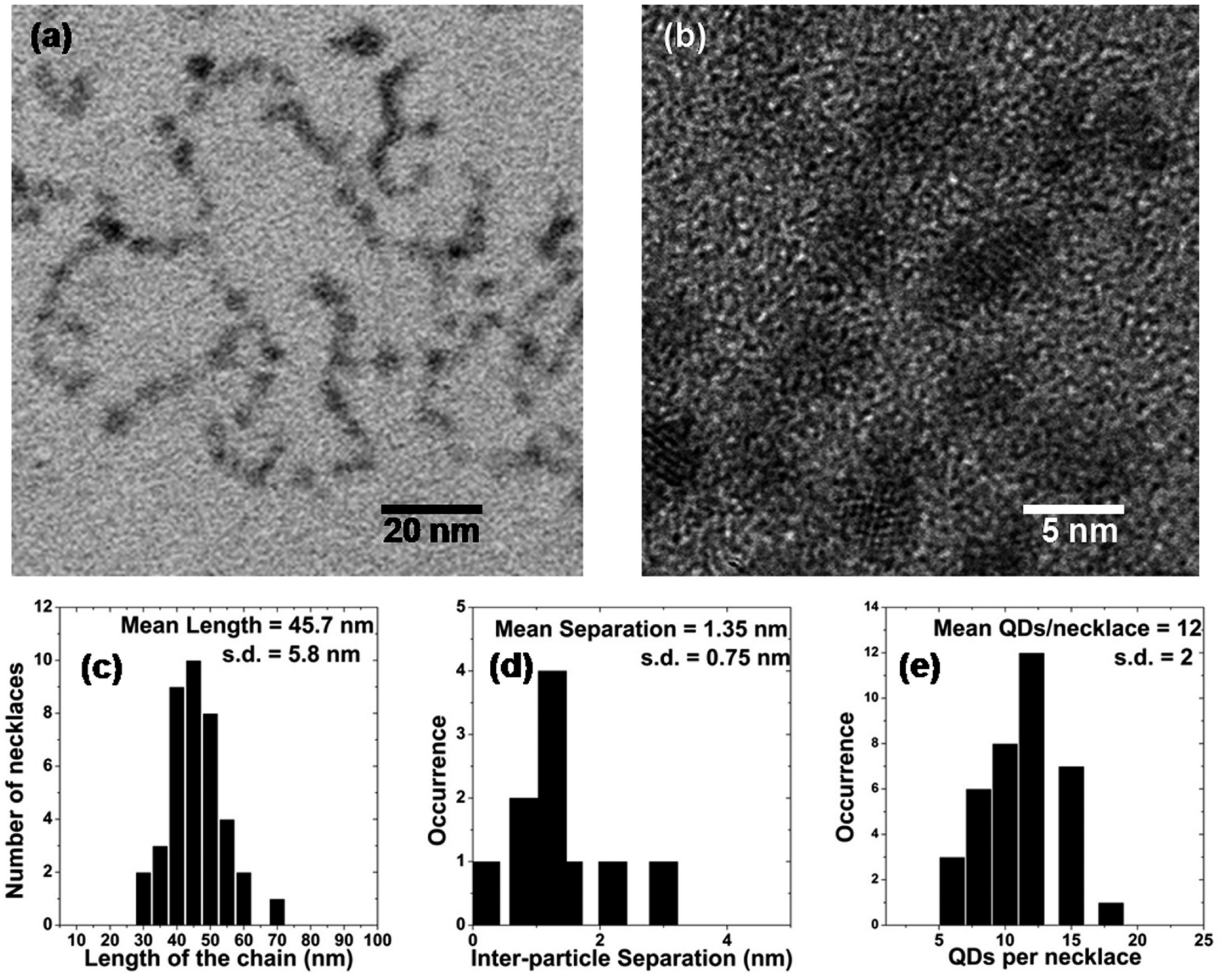

Figure 5. (a) TEM image of HgTe nanonecklaces formed by keeping G7 dendrimer-encapsulated nanoparticles in the dark at 10 °C. These results are typical for samples stored for at least 3 weeks. (b) High-resolution TEM image showing interparticle spacing typical of HgTe nanonecklaces. (c−e) Histograms showing the chain length distribution (c), mean separation between QDs (d), and number of QDs per necklace (e).

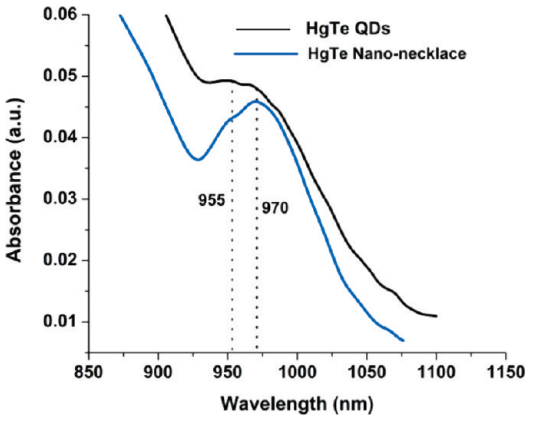

Figure 6. Near-infrared absorption spectra of HgTe QDs and HgTe nanonecklaces.

diameter of the G7 dendrimer is 8.5 nm;[41] this value remains unchanged when a HgTe QD is introduced into the dendrimer's internal void space. Scheme 1 shows the three possible ways in which two dendrimer-encapsulated QDs can be placed close to each other. In Scheme 1a, the two QDs touch each other, thus accounting for some of the inter-QD separation. However, we note that ~70% of observed inter-QD separations were in the range of 0.5−1.5 nm (Figure 5c). If the dendrimer-encapsulated QDs were placed in a manner similar to that shown in panel b or c of Scheme 1, the anticipated inter-QD separation would be ~5 or ~10 nm, respectively. These values are not consistent with the available TEM data for the HgTe necklaces. A smaller inter-QD separation could be achieved if the HgTe QDs were partially expelled from the dendrimer cavity as it approached a neighboring particle. In Scheme 1b, the two dendrimers do not touch each other solely at the periphery. Rather, the dendritic arms intercolate, thus reducing the distance between two adjacent QDs. In this case, the extent of interpenetration would determine the inter-QD separation. The possibility for the population of a species giving rise to the experimentally determined separations reported in panels c and d of Figure 5 that spanned the range of 0.5−1.5 nm cannot be excluded. This assembly mechanism should lead to a significant difference between the FTIR spectra of the free and nanonecklace-assembled HgTe QDs. Indeed, a distinct change in FTIR spectral position was observed for the stretching vibrations of surface amines; this peak was blue-shifted by 30 cm^{-1} as displayed in Figure 7a. However, no differences in the positions or fwhm of the peaks corresponding to the interior amide I and amide II vibrations (1563 and 1630 cm^{-1}, respectively) were observed. The latter result indicated that the integrity of the dendritic encapsulation of HgTe QDs was not compromised during the process of self-assembly from dots to necklaces.

Scheme 1. Illustration of How the Dendrimer-Encapsulated QDs Can Be Placed Together in a Necklace Pattern To Achieve Different Inter-QD Separation (d_{QD})[a]

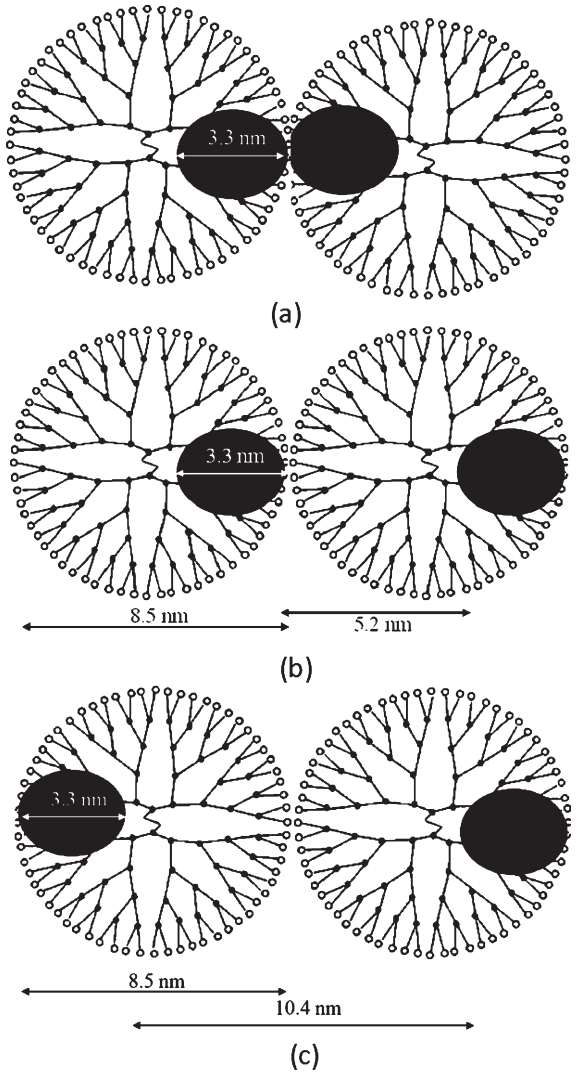

[a] (a) d_{QD} = 0 nm. (b) d_{QD} = 5.2 nm. (c) d_{QD} = 10.4 nm.

The differences in the stretching vibrations of surface amines became more apparent upon examination of the second-derivative spectra and the corresponding deconvoluted peaks in the 3000−3700 cm^{-1} region (Figure 7b). In comparison to the dendrimer-encapsulated QDs (Figure 4b), the relative intensity of the 3,3′ peak was decreased further in the necklaces. The FTIR data indicated that the interaction of surface amines with HgTe had become stronger in necklaces than in dendrimer-encapsulated quantum dots. This finding suggested a self-assembly mechanism that involves interpenetration of dendritic arms from neighboring dendrimer-encapsulated QDs, as illustrated in Scheme 1c. In such a scenario, the free surface amines of one dendrimer can interact with the HgTe QD in the cavity of another dendrimer, causing a decrease in the intensity of the N−H stretch (3,3′ peak). Thus, necklace assembly appears to be driven by the strong affinity of surface amines for the cationic sites on the HgTe surface. It should be noted that the binding of amines to the Hg(II) sites on the surface of HgTe particles is much stronger than the binding of these same amine groups to the Hg^{2+} ions in solution. This was clearly evident in the FTIR spectra shown in Figures 3 and 8. Addition of Hg^{2+} ions to the dendrimer solution did not change

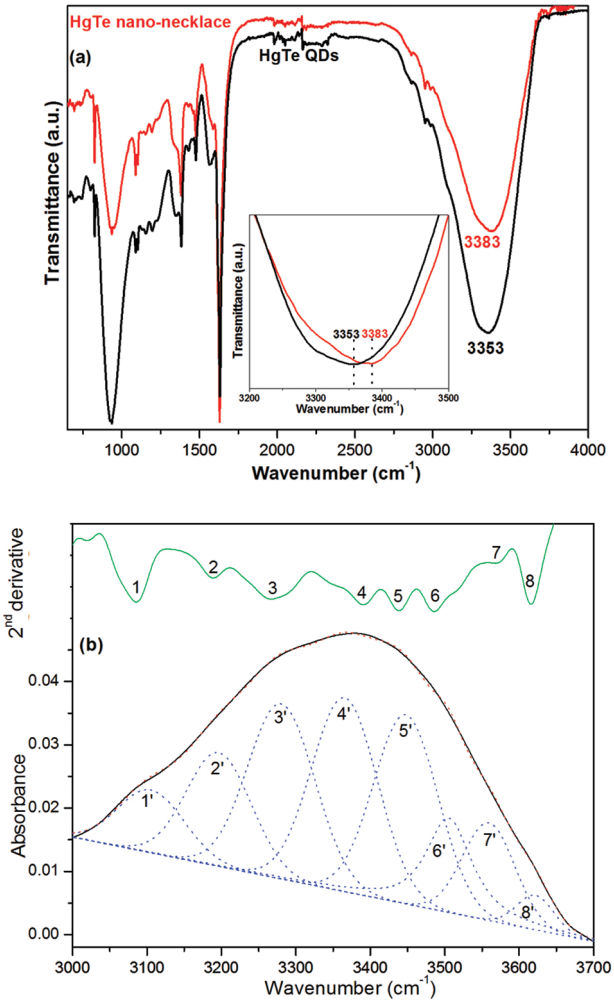

Figure 7. (a) FTIR spectra of dendrimer-encapsulated HgTe QDs and HgTe nanonecklaces. The inset shows the zoomed-in view of the 3200−3500 cm^{-1} region. (b) Deconvolutions of FTIR spectra (3000−3700 cm^{-1}region) of the dendrimer−HgTe nanonecklace: (black line) raw FTIR data, (blue dots) deconvoluted peaks, (red dots) overall fitting, and (green line) second-derivative plot. Band assignments of deconvolutions: 1,1′, overtone of amide II;[50] 2,2′, H-bonded N−H stretch;[49] 3,3′-N−H symmetric stretch;[43,47,49,50] 4,4′, N−H asymmetric stretch;[47] 5,5′, amide A vibrations (N−H stretch of amide);[47] 6,6′, O−H stretch;[49] 7,7′ and 8,8′, HgTe-bonded N−H stretch.

the FTIR spectra in the 3000−3700 and 1515−1785 cm^{-1} regions (Figure 8). By contrast, changes in these spectroscopic regions were easily perceptible after the formation of HgTe particles as discussed in earlier sections.

In the process of necklace formation, as the neighboring dendrimers interpenetrated, enhanced hydrogen bonding interactions became possible between the dendritic arms through interior amide bonds. Upon careful examination of the spectrum shown in Figure 6a, we did find a substantial change in the ratios of integrated intensities for amide I to amide II peaks (1:6 in the QDs and 1:9 in the necklaces). A ratio shift of this magnitude has been previously attributed to hydrogen bonding interactions;[43,44] a similar assessment was made here for the HgTe necklaces. In essence, there are two factors that govern the self-assembly of HgTe QDs into HgTe necklaces: (i) interdigitation and binding of terminal dendrimer NH_2 groups to the HgTe surface of the neighboring particle and (ii) enhanced hydrogen bonding between the dendritic arms. Both factors decrease the free energy

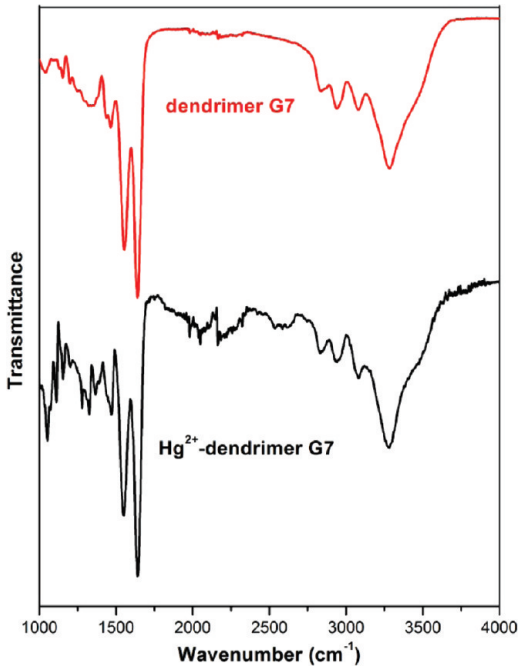

Figure 8. FTIR spectra of the PAMAM G7 dendrimer before (red) and after (black) addition of Hg^{2+} ions.

of the dendrimer−HgTe system, thereby making the process spontaneous.

The dendrimer architecture also plays a role in the assembly. It has been shown[31] that a dendritic chain that is either too rigid or too flexible can prevent reorganization of QDs into such well-defined 2D nanostructures. The G7 dendrimers used here appeared to possess an appropriate level of rotomeric freedom that favored formation of nanonecklaces.

4. Conclusion

We report the synthesis of very stable and highly monodisperse dendrimer-encapsulated HgTe QDs by careful optimization of key parameters: dendrimer generation, concentration, and temperature. Although G5 dendrimers provided the most monodisperse HgTe QDs, the G7 product exhibited the best long-term stability, exceeding one year. The improved stability of the G7-encapsulated nanoparticles was attributed to the larger number of available amine functional groups in a single dendrimer to passivate the QD surface. The importance of G7 dendrimers was further illustrated by the unique self-organizing ability exhibited by the encapsulated quantum dots. In the nanonecklaces, the individual identity of QDs was retained, but evidence indicated that close packing of the nanoparticles resulted in electronic coupling. The large optical absorption cross section predicted for such strongly coupled systems could serve as a platform for enhanced light absorption centers in photovoltaic devices. In addition, tailoring of the hydrogen bonding network between neighboring dendrimers in self-assembled structures may allow for rational design of 2D nanostructures with well-defined geometry.

Acknowledgment. K.L.K. gratefully acknowledges funding from the Air Force Office of Scientific Research. We also acknowledge the Florida State University Research Foundation and the Florida State University CRC for financial support. TEM work was carried out using the facility at the National High Magnetic Field Laboratory supported by National Science Foundation Cooperative Agreement DMR-0084173, with the State of Florida.

Supporting Information Available: Near-infrared absorption spectra of HgTe QDs synthesized at different temperature using the PAMAM G5 dendrimer (Figure S1), high-resolution TEM image of HgTe nanonecklaces (Figure S2), optical properties of HgTe QDs synthesized with the PAMAM G5 dendrimer in methanol at 5 °C (Table S1), and positions and areas of the deconvoluted IR aborption peaks in the region of 3000−3700 cm^{-1} (Table S2). This material is available free of charge via the Internet at http://pubs.acs.org.